Comment on "Estimating the depth and evolution of intrusions at resurgent calderas: Los Humeros (Mexico)" by Urbani et al. (2020)

Gianluca Norini[1], Gianluca Groppelli[1]

[1]Istituto di Geologia Ambientale e Geoingegneria, Sezione di Milano, Consiglio Nazionale delle Ricerche, Italy

Correspondence to: Gianluca Norini (gianluca.norini@cnr.it)

Abstract. A multiple shallow–seated magmatic intrusions model has been proposed by Urbani et al. (2020) for the resurgence of the Los Potreros caldera floor, in the Los Humeros Volcanic Complex. This model predicts (1) the occurrence of localized bulges in the otherwise undeformed caldera floor, and (2) that the faults corresponding to different bulges exhibit different spatial and temporal evolution. Published data and a morphological analysis show that these two conditions are not met at Los Potreros caldera. A geothermal well (H4), located at the youngest supposed bulge (Loma Blanca) for which Urbani et al. (2020) calculated an intrusion depth (425±170 m), doesn't show any thermal and lithological evidence of such a shallow–seated cryptodome. Finally, published stratigraphic data and radiometric dating disprove the proposed common genesis of Holocene resurgence faulting and viscous lavas extruded in the centre of the caldera. Even if recent shallow intrusions may exist in the area, published data indicate that the pressurization of the LHVC magmatic/hydrothermal system driving resurgence faulting occurs at greater depth. Thus, we suggest that the model and calculation proposed by Urbani et al. (2020) are unlikely to have any relevance to the location, age and emplacement depth of magma intrusions driving resurgence at the Los Potreros caldera.

1 Introduction

Urbani et al. (2020) (henceforth U2020) made a contribution to the study of caldera resurgence based on field data and geothermal well logs from the Los Humeros Volcanic Complex (LHVC) and scaled analogue models. U2020 constrained the spatial–temporal evolution of post–caldera volcanism at LHVC and estimate the depth of the magmatic intrusions feeding the active geothermal system by integrating fieldwork data, well logs and laboratory results. The main conclusion of U2020 is that the resurgence of the Los Potreros caldera in the LHVC "*is due to multiple deformation sources*", "*linked to small magmatic intrusions located at relatively shallow depths (i.e. < 1 km)*". U2020 suggested that these intrusions are located below three uplifted areas surrounding the Arroyo Grande, Los Humeros and Loma Blanca faults, respectively.

The analysis by U2020 suffers from poor field data and contradictions with thermal remote sensing data (Section 2), geometric and structural inconsistencies between the LHVC post–caldera deformation and the analogue modelling (Section 3), lack of any substantial validation of the results with published well logs (Section 4), and incongruities with the reference stratigraphy and radiometric ages recently published by some of the U2020 authors (Section 5). These problems, which largely undermine the U2020 conclusions, are discussed below.

2 Location and relative age of faulting: field data and thermal remote sensing

U2020 analysed the occurrence and relative age of faulting, and proposed a new interpretation of some structures identified by previous works, by studying faults and hydrothermal alteration in the Holocene Cuicuiltic Member unit (Ferriz and Mahood, 1984; Arellano et al., 2003; Dávila–Harris and Carrasco–Núñez, 2014; Norini et al., 2015, 2019). The Cuicuiltic Member blankets the Los Potreros caldera floor (Fig. 1), is very well exposed, has been dated at ca. 7 ka and is made of alternated fallout deposits of different composition (Dávila–Harris and Carrasco–Núñez, 2014). The Cuicuiltic Member has been considered an ideal marker layer for documenting Holocene faulting and stratigraphy in the

caldera complex, because of the contrasting black and white colours of the fallout deposits composing the unit (e.g. Ferriz and Mahood, 1984; Dávila–Harris and Carrasco–Núñez, 2014; Norini et al., 2015, 2019; GEMex, 2019; U2020) (Figs. 1 and 2). The reinterpretation by U2020 has been based on their field data (22 fault data in 3 outcrops), distinguishing between lineaments ("*morphological linear scarps with no measurable fault offsets and/or alteration at the outcrop scale*") and active and inactive faults ("*associated with measurable fault offsets and with active or fossil alteration*"), respectively. The reinterpreted structures are the Las Papas, Las Viboras, Arroyo Grande and Maxtaloya faults (Fig. 1).

We discuss the U2020 reinterpretation below, considering published field data (175 fault data in 24 outcrops, Figs. 1 and 2, Tab. 1) and thermal remote sensing data (Fig. 3) (Norini et al., 2015, 2019; GEMex, 2019).

2.1 Las Papas and Las Viboras faults

U2020 concluded that the Las Papas and Las Viboras are "*morphological scarps*" and "*lineaments*" not related to faulting. For the Las Papas lineament, U2020 stated that "*unaltered and undeformed deposits of the Cuicuiltic Member crop out along the E–W Las Papas lineament*" and that it "*is probably due to differential erosion of the softer layers of the pyroclastic deposits*". Even if the Las Papas and Las Viboras structures were several km long, the statements by U2020 have only been based on one outcrop on the Las Papas trace (U2020 LH–08 outcrop, while the LH–07 outcrop is out of the fault trace; see Fig. 4C).

Several outcrops exist along the Las Papas and Las Viboras faults, as well as along many other faults in the area surrounding these two main volcanotectonic structures (Fig. 1) (e.g. Dávila–Harris and Carrasco–Núñez, 2014; Norini et al., 2015, 2019; GEMex, 2019). In all these outcrops, the faults invariably displace the Holocene Cuicuiltic Member and the underlying lava and pyroclastic units (Figs. 1 and 2; Tab. 1). These data (Tab. 1) are incompatible with the U2020 conclusion that the Las Papas and Las Viboras are not faults. Indeed, the data indicate that the Las Papas and Las Viboras structures have been originated in the Holocene by faulting (Figs. 1 and 2, and Tab. 1) (Dávila–Harris and Carrasco–Núñez, 2014; Norini et al., 2015, 2019; GEMex, 2019). The U2020 description of their LH–08 outcrop can be explained by erosive retreat of the fault scarp, a common process in dip–slip faults, especially in poorly consolidated sediments (e.g. Keller and Pinter, 2002; Burbank and Anderson, 2011).

2.2 Arroyo Grande and Maxtaloya faults

U2020 inferred that the Arroyo Grande and Maxtaloya scarps have been generated by nowadays inactive faults. U2020 stated that these faults have been active "*prior to the deposition of the Cuicuiltic Member*". The statement by U2020 arose from the analysis of two outcrops (their LH–09, see Fig. 4C, and the H6 well pad, corresponding to the PDL08 outcrop of Figs. 1 and 2H), where "*strongly altered and faulted ... lavas and ignimbrites*" are "*covered by the unaltered Cuicuiltic Member*". Active/fossil alteration doesn't always allow identifying faults or the age of faulting, because it depends also on their depth, life span of the hydrothermal system, spatial relationships, and fluid paths along primary permeability and fracture zones (e.g. Bonali et al., 2016; Giordano et al., 2016).

Outcrops of the Arroyo Grande and Maxtaloya faults show displacements of the Cuicuiltic Member, which are incompatible with the conclusion of U2020 about the age of these two structures and the correlation between faulting and hydrothermal alteration (Figs. 1 and 2; Tab. 1). The field data (Figs. 1 and 2, and Tab. 1) indicate that the Arroyo Grande and Maxtaloya faults have been active after the deposition of the Cuicuiltic Member (Dávila–Harris and Carrasco–Núñez, 2014; Norini et al., 2015, 2019; GEMex, 2019).

The Maxtaloya fault trace is coincident with a sharp thermal anomaly identified by Norini et al. (2015) (Fig. 3). U2020 didn't consider this positive (warm) anomaly when they discussed the thermal remote sensing results published by Norini et al. (2015) (Section 5.3 in U2020). The thermal remote sensing data (Fig. 3) suggest that the Maxtaloya fault plays nowadays an important role in the ascent of hot geothermal fluids (Norini et al., 2015, 2019; Carrasco–Núñez et al., 2017; GEMex, 2019).

The Maxtaloya positive thermal anomaly constitutes the southern branch of a narrow warm corridor (T1 of Norini et al., 2015), which is spatially coincident with the NNW–SSE fault swarm represented by the Maxtaloya fault, Los Humeros

90 fault and some sub–parallel normal and reverse fault strands (Fig. 3) (Norini et al., 2019). This 7–8 km–long thermal
91 anomaly is incompatible with the presence of the "*shallow and delocalized heat sources*" proposed by U2020 (Fig. 3).
92 Instead, the great length of this narrow thermal anomaly is consistent with a deeper pressure source driving resurgence
93 faulting (e.g. an asymmetric cup-shaped intrusion), with lower surface temperatures in the centre of the thick resurgent
94 block (cold area to the east of the 7–8 km–long warm anomaly in Fig. 3) (see Norini et al., 2015).

95

96 **3 Identification and geometry of uplifted areas: topographic data and structural mapping**

97 U2020 identified three "*main uplifted areas*" surrounding the surface expressions of the Loma Blanca, Arroyo Grande
98 and Los Humeros faults. U2020 didn't provide any information on how these uplifted areas have been identified and
99 delimited with specific and reproducible criterion. The area around the Loma Blanca fault has been named by U2020
100 "*Loma Blanca bulge*" and described as "*a morphological bulge, 1 km in width and 30 m in height*". The U2020 model
101 also predicts the formation of an "*apical depression*" on top of a "*bulge*" induced by a shallow magmatic intrusion. Indeed,
102 U2020 depicted apical depressions on top of the three "*uplifted areas*" of Loma Blanca, Arroyo Grande and Los Humeros
103 (e.g. cross–sections in Fig. 10 by U2020).

104 Topographic profiles of the Los Potreros caldera floor extracted from a 1 m resolution Digital Elevation Model (DEM)
105 (Norini et al., 2019) show that the "*uplifted areas*" (or "*bulges*") identified by U2020 include asymmetric reliefs and
106 depressed sectors, and have boundaries not necessarily corresponding to slope changes useful for their delimitation (Figs.
107 1 and 4A-C). The "*Loma Blanca bulge*" defined by U2020 comprises a sector of a larger and uniform westward tilted and
108 faulted surface (Norini et al., 2019). The western boundary of the "*bulge*" is in the middle of the tilted surface, while the
109 eastern one, corresponding to a normal fault, is nearly at the same elevation of the summit of the "*bulge*" (Figs. 1 and 4A)
110 (Carrasco–Núñez et al., 2017; Norini et al., 2019). Similarly, the eastern and western boundaries of the Arroyo Grande
111 and Los Humeros "*uplifted areas*" have been located by U2020 in the middle of tilted or flat surfaces. The topographic
112 data extracted from the 1 m resolution DEM (Figs. 1 and 4A–B) are incompatible with the occurrence of the "*main
113 uplifted areas*" or "*bulges*" identified by U2020. The same topographic data are also incompatible with the occurrence of
114 any "*apical depression*" along the Arroyo Grande and Los Humeros faults, suggesting that the present topography of the
115 caldera floor doesn't have any relation with the "*uplifted areas*", "*bulges*" and "*apical depressions*" presented by U2020
116 (Figs. 1 and 4A-C).

117 The analogue modelling by U2020 predicts the development of reverse faults at the base of the "*bulges*" induced by the
118 emplacement of shallow–seated cryptodomes (e.g. Fig. 7 by U2020). U2020 didn't provide any field data or other
119 evidence (morphostructural interpretation, geophysics, well logs, etc.) locating these reverse faults, which are a
120 fundamental feature of their model. Reverse faults of this type have been identified in natural cases of shallow–seated
121 intrusions (e.g. Sibbett, 1988; Jackson and Pollard, 1990; Schofield et al. 2010; Wilson et al. 2016).

122 Structural maps of the Los Potreros caldera published by Carrasco–Núñez et al. (2017); Calcagno et al. (2018); Norini et
123 al. (2019) and U2020 are inconsistent with the idea of reverse faults at the base of the "*bulges*" identified by U2020 (Figs.
124 1 and 4C). The "*Loma Blanca bulge*" is delimited to the east by a normal fault mapped by Carrasco–Núñez et al. (2017)
125 and Norini et al. (2019) (Fig. 4A).

126

127 **4 Validation of the proposed model: geothermal wells log data**

128 One of the most significant findings of U2020 is that the uplift in the "*Loma Blanca bulge*" has been generated by a
129 magmatic intrusion located at 425 ± 170 m of depth. U2020 also stated that this is the heat source of the local geothermal
130 anomaly. Such a shallow depth is within the range of geothermal wells drilled in the area. A validation attempt of the
131 U2020 model in the "*Loma Blanca bulge*" consists in the comparison of the temperature and lithological H4 well log with
132 the predicted intrusion depth. This well is located at the top of the "*bulge*", just to the west of its "*apical depression*" (Fig.
133 4A,C). The H4 well log should show a significant temperature change and intrusive/sub–volcanic lithologies at 425 ± 170
134 m of depth, if a shallow–seated, still hot magmatic intrusion exists beneath the "*Loma Blanca bulge*".

135 According to data published by Arellano et al. (2003) and U2020, the H4 stratigraphic log doesn't show any evidence of
136 intrusive bodies from the surface down to 1900 m of depth, nor a sharp increase of the temperature and geothermal

137 gradient, which remains constant (about 20°C/100 m) (Fig. 4D). Also, the temperature profiles measured in several wells
138 of the field (e.g. Arellano et al., 2003) don't show any strong temperature inversion or sharp change in the geothermal
139 gradient possibly correlated to recent intrusive bodies at very shallow depth ("< *1 km*"), nor any shallow–seated
140 intrusive/sub–volcanic lithology (Cavazos-Álvarez et al., 2020). Lithological well logs show the presence of rhyolitic–
141 andesitic rock layers within the Caldera group (mainly in the Xaltipan ignimbrite unit; Carrasco–Núñez et al., 2017),
142 which have been interpreted by U2020 as "*intrusion of felsic cryptodomes within the volcanic sequence*". A recent study
143 of these felsic layers, based on petrographic and geochemical analyses of borehole samples, identified them as "*lithic-*
144 *rich breccias of local and irregular distribution that formed during the caldera collapse event*" (Cavazos-Álvarez et al.,
145 2020).

146 Published well log data indicate a deeper origin of the heat source (or sources) feeding the Los Humeros geothermal field,
147 with some variation of the temperature gradient due to faults and or permeability changes (Fig. 4D) (e.g. Cedillo et al.,
148 1997; Arellano et al., 2003; Cavazos-Álvarez et al., 2020).
149

5 Validation of the proposed model: stratigraphic and radiometric data

151 One of the results presented in U2020 is that "*...the recent (post–caldera collapse) uplift in the Los Potreros caldera*
152 *moved progressively northwards ... along the Los Humeros and Loma Blanca scarps*". Based on the proposed U2020
153 uplift model, it suggests that shallow intrusions of small magmatic bodies and, consequently, the volcanic feeding system
154 moved progressively northwards. This statement presents some discrepancies with the stratigraphy, geological mapping
155 and radiometric ages published recently (Carrasco–Núñez et al., 2017, 2018; Juárez–Arriaga et al., 2018), as summarised
156 by the following points:

157 a) An obsidian dome (Qr1 Rhyolite of Carrasco–Núñez et al., 2017) has been dated using the U/Th method at
158   44.8±1.7 ka by Carrasco–Núñez et al. (2017, 2018). Its location corresponds to the obsidian dome cropping out
159   along the Los Humeros fault described in U2020 and connected with the syn– to post–Cuicuiltic Member
160   eruption (7.3–3.8 ka) (Fig. 5). In U2020 there is no description of two generations of obsidian domes along Los
161   Humeros fault, nor any explanation to invalidate the previous radiometric dating. Therefore, the U2020
162   attribution of this obsidian dome to the 7.3–3.8 ka volcanic activity phase appears unjustified and, consequently,
163   weakens their model;

164 b) The most recent volcanic activity of LHVC (post–Cuicuiltic Member) is clustered in two main ages, around 3.8
165   and 2.8 ka, as indicated by recent radiometric and paleomagnetic data (Carrasco–Núñez et al., 2017; Juárez–
166   Arriaga et al., 2018) (Fig. 5). According to these ages and the LHVC geological map (Carrasco–Núñez et al.,
167   2017), the vents feeding the post–Cuicuiltic Member volcanic activity are mainly located close to the southern
168   and south–western sectors of the Los Humeros caldera rim. These data suggest that the shallow feeding system
169   of the post–Cuicuiltic Member activity is mainly located in the southern and south–western sectors of the LHVC,
170   some kilometres far from the supposed bulged areas. Also, the ages and locations of the volcanic vents do not
171   show any progressive northward shift, but a scattered activity along the Los Humeros caldera rim.
172

6 Conclusion

174 We identified several problems in the U2020 study, showing that their model does not conform to most of the published
175 geological data about the Los Potreros caldera. The boundary conditions of a model and the validation of the modelling
176 results should always be based on the geological constraints that the natural prototype imposes. In our opinion, the
177 multiple magmatic intrusion model is imposed by U2020 to the natural prototype regardless of several evidences of no
178 fit between them. This mismatch between nature and model includes the age and location of faulting, identification and
179 delimitation of uplifted areas and apical depressions, temperature and lithological wells log, and stratigraphic and
180 radiometric data. The occurrence of multiple magmatic intrusions at different depths in the Los Potreros caldera is not
181 questioned in our comment. Published data indicate that the calculations and conclusions by U2020 are unlikely to have
182 any relevance to the identification of the deformation source driving caldera resurgence and the heat source feeding the
183 geothermal field. The data and interpretations discussed in our comment have scientific and economic implications.

184 Indeed, they are important to plan the best strategies for geothermal exploration and production, reducing drilling risk
185 and potential loss of investment.
186
187

188 **Data availability:** all the data presented in this paper are available upon request.

189 **Author contributions:** Gianluca Norini and Gianluca Groppelli are equally responsible for *Conceptualization* (research
190 planning), *Investigation* (field analysis, geomorphological analysis, review of well logs and stratigraphic data), *Writing -*
191 *Original Draft* and *Review & Editing*, and *Visualization* (figures and maps).

192 **Competing interests:** the authors declare that they have no conflict of interest.

199 **References**
200 Arellano, V.M., Garcia, A., Barragan, R.M., Izquierdo, G., Aragon, A., Nieva, D., 2003. An updated conceptual model
201 of the Los Humeros geothermal reservoir (Mexico). J. Volcanol. Geotherm. Res. 124, 67–88.

202 Bonali, F., Corazzato, C., Bellotti, F., and Groppelli, G. (2015). Active tectonics and its interactions with Copahue
203 volcano. In F. Tassi, O. Vaselli, & A.T. Caselli (eds.), Copahue Volcano, Springer, Berlin Heidelberg, 23–45.

204 Burbank D.W. and Anderson R.S. (2011). Tectonic Geomorphology. Second Edition, John Wiley & Sons, Ltd,
205 Chichester, UK. 274 pp.

206 Calcagno, P., Evanno, G., Trumpy, E., Gutiérrez-Negrín, L. C., Macías, J. L., Carrasco-Núñez, G., and Liotta, D., 2018,
207 Preliminary 3-D geological models of Los Humeros and Acoculco geothermal fields (Mexico)–H2020 GEMex Project:
208 Advances in Geosciences, v. 45, p. 321.

209 Carrasco–Núñez, G., Hernández, J., De León, L., Dávila, P., Norini, G., Bernal, J.P., Jicha, B., Navarro, M., López–
210 Quiroz, P., and Digitalis, T.: Geologic Map of Los Humeros volcanic complex and geothermal field, eastern Trans–
211 Mexican Volcanic Belt, Terra Digitalis, 1, 1–11, https://doi.org/10.22201/igg.terradigitalis.2017.2.24.78, 2017.

212 Carrasco–Núñez, G., Bernal, J. P., Davila, P., Jicha, B., Giordano, G., and Hernández, J.: Reappraisal of Los Humeros
213 volcanic complex by new U/Th zircon and 40Ar/39Ar dating: Implications for greater geothermal potential, Geochem.
214 Geophy. Geosy., 19, 132–149, 2018.

215 Cavazos-Álvarez J.A., Carrasco-Núñez G., Dávila-Harris P., Peña D., Jáquez A., Arteaga D. (2020). Facies variations
216 and permeability of ignimbrites in active geothermal systems; case study of the Xáltipan ignimbrite at Los Humeros
217 Volcanic Complex. Journal of South American Earth Sciences, 104, 102810.

218 Cedillo, F., 1997. Geologia del subsuelo del campo geotermico de Los Humeros, Pue. Internal Report HU/RE/03/97,
219 Comision Federal de Electricidad, Gerencia de Proyectos Geotermoelectricos, Residencia Los Humeros, Puebla, 30 pp.

220 Dávila–Harris, P. and Carrasco–Núñez, G.: An unusual syn–eruptive bimodal eruption: The Holocene Cuicuiltic Member
221 at Los Humeros caldera, Mexico, J. Volcanol. Geoth. Res., 271, 24–42, https://doi.org/10.1016/j.jvolgeores.2013.11.020,
222 2014.

223 Ferriz, H., Mahood, G., 1984. Eruptive rates and compositional trends at Los Humeros volcanic center, Puebla, Mexico.
224 J. Geophys. Res. 89, 8511–8524.

225 GEMex (2019). Final report on active systems: Los Humeros and Acoculco. Deliverable 4.1. GEMex project technical
226 report, Horizon 2020, European Union, 334 pp. www.gemex–h2020.eu.

227 Giordano G., Ahumada F., Aldega L., Baez W., Becchio R., Bigi S., Caricchi C., Chiodi A., Corrado S., De Benedetti A.,
228 Favetto A., Filipovich R., Fusari A., Groppelli G., Invernizzi C., Maffucci R., Norini G., Pinton A., Pomposiello C., Tassi
229 F., Taviani S., Viramonte J. (2016). Preliminary data on the structure and potential of the Tocomar geothermal field (Puna
230 plateau, Argentina). Energy Procedia, 97, 202–209.

231 Jackson M.D., Pollard D.D.: Flexure and faulting of sedimentary host rocks during growth of igneous domes, Henry
232 Mountains, Utah, Journal of Strucctural Geology, 12 (2), 185-206, 1990.

233 Juárez-Arriaga, E., Böhnel, H., Carrasco–Núñez, G., Nasser Mahgoub, A. (2018). Paleomagnetism of Holocene lava
234 flows from Los Humeros caldera, eastern Mexico: Discrimination of volcanic eruptions and their age dating. Journal of
235 South American Earth Sciences, 88, 736-748.

236 Keller, E.A. and Pinter, N. (2002). Active Tectonics: Earthquakes, Uplift, and Landscape. Second Edition. Prentice Hall,
237 Upper Saddle River, 361 pp.

238 Norini, G., Groppelli, G., Sulpizio, R., Carrasco–Núñez, G., Dávila–Harris, P., Pellicioli, C., Zucca, F., and De Franco,
239 R.: Structural analysis and thermal remote sensing of the Los Humeros Volcanic Complex: Implications for volcano
240 structure and geothermal exploration, J. Volcanol. Geoth. Res., 301, 221–237,
241 https://doi.org/10.1016/j.jvolgeores.2015.05.014, 2015.

242 Norini, G., Carrasco–Núñez, G., Corbo–Camargo, F., Lermo, J., Hernández Rojas, J., Castro, C., Bonini, M., Montanari,
243 D., Corti, G., Moratti, G., Chavez, G., Ramirez, M., and Cedillo, F.: The structural architecture of the Los Humeros
244 volcanic complex and geothermal field, J. Volcanol. Geoth. Res., 381, 312–329,
245 https://doi.org/10.1016/j.jvolgeores.2019.06.010, 2019.

246 Schofield, N., Stevenson, C., & Reston, T. Magma fingers and host rock fluidization in the emplacement of sills. Geology,
247 38(1), 63-66, 2010.

248 Sibbett, B.S. Size, depth and related structures of intrusions under stratovolcanoes and associated geothermal systems.
249 Earth-Sci. Rev., 25: 291-309, 1988.

250 Urbani, S., Giordano, G., Lucci, F., Rossetti, F., Acocella, V., and Carrasco–Núñez, G.: Estimating the depth and
251 evolution of intrusions at resurgent calderas: Los Humeros (Mexico), Solid Earth, 11, 527–545,
252 https://doi.org/10.5194/se–11–527–2020, 2020.

253 Wilson P.I.R., McCaffrey K.J.W., Wilson R.W., Jarvis I., Holdsworth R.E. Deformation structures associated with the
254 Trachyte Mesa intrusion, Henry Mountains, Utah: Implications for sill and laccolith emplacement mechanisms, Journal
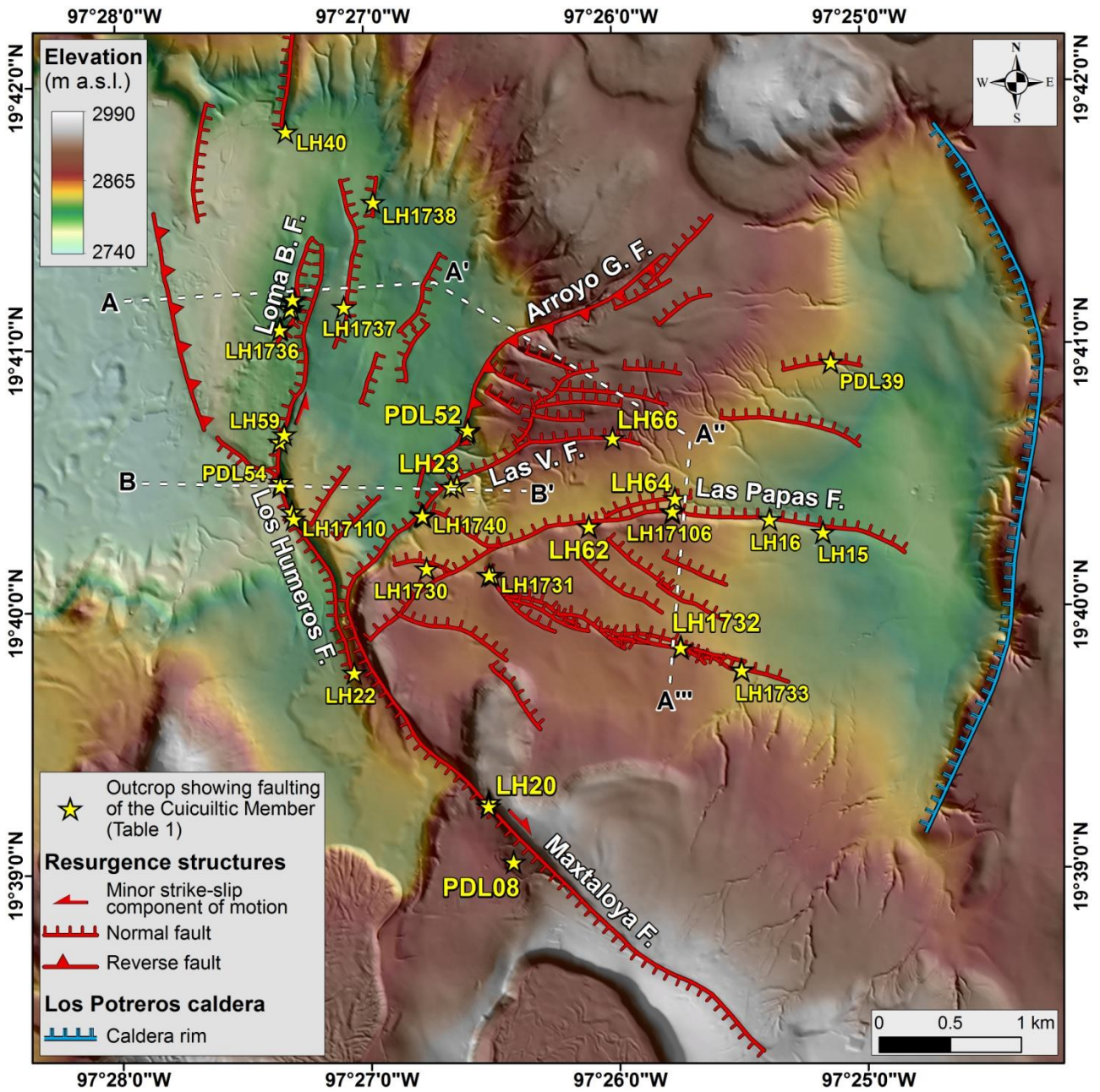255 of Structural Geology, 87, 30-46, https://doi.org/10.1016/j.jsg.2016.04.001, 2016.

256

257

258

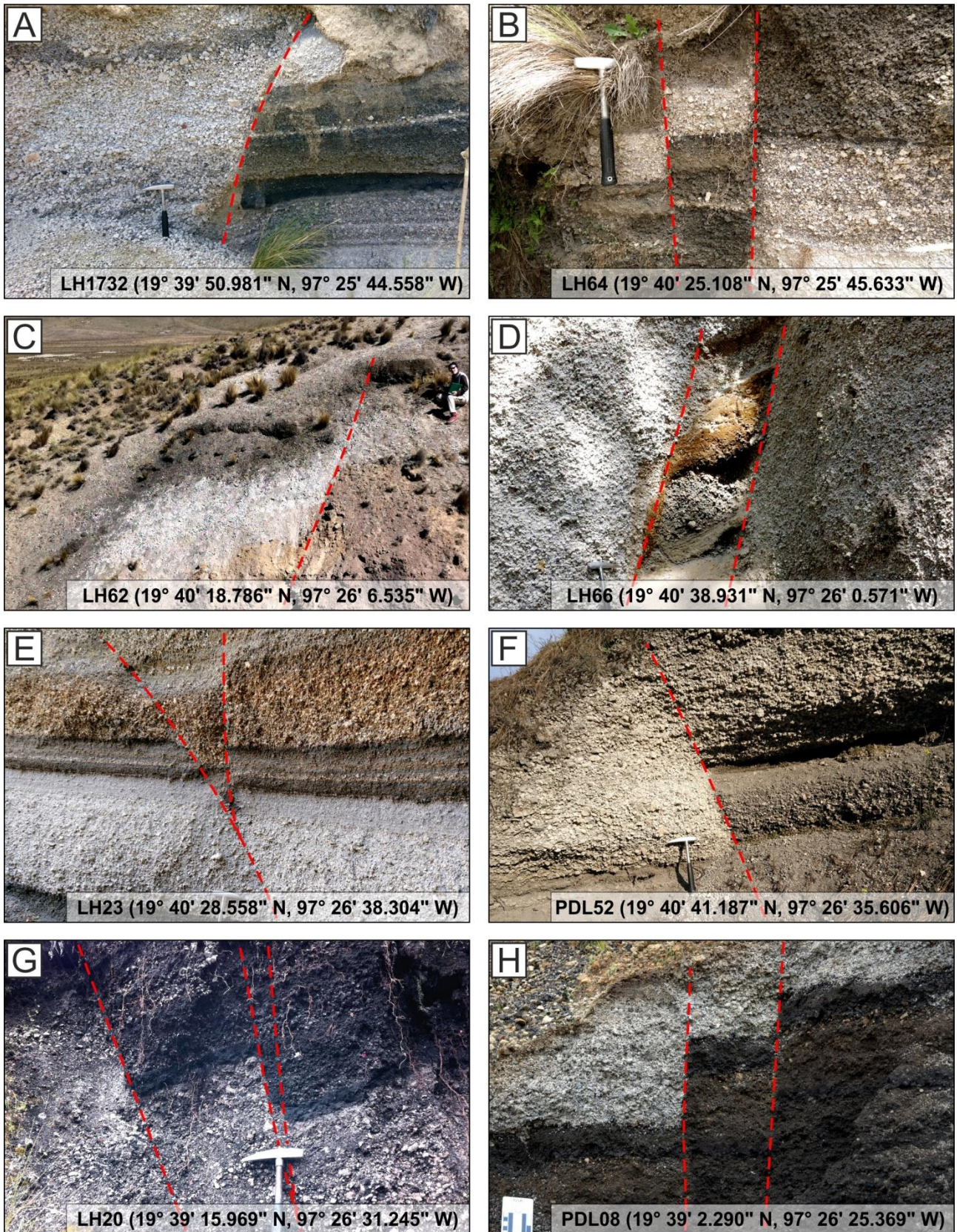259

260

261

Figure 1: volcanotectonic map of the Los Potreros caldera area, on a DEM (illuminated from the E) (modified from GEMex, 2019 and Norini et al., 2019). Las V.F.: Las Viboras fault; Arroyo G.F.: Arroyo Grande fault; Loma B.F.: Loma Blanca fault. Location of outcrops in Fig. 2 and Tab. 1 is shown. Traces of A–A'–A''–A''' and B–B' topographic profiles of Fig. 4 are also shown.
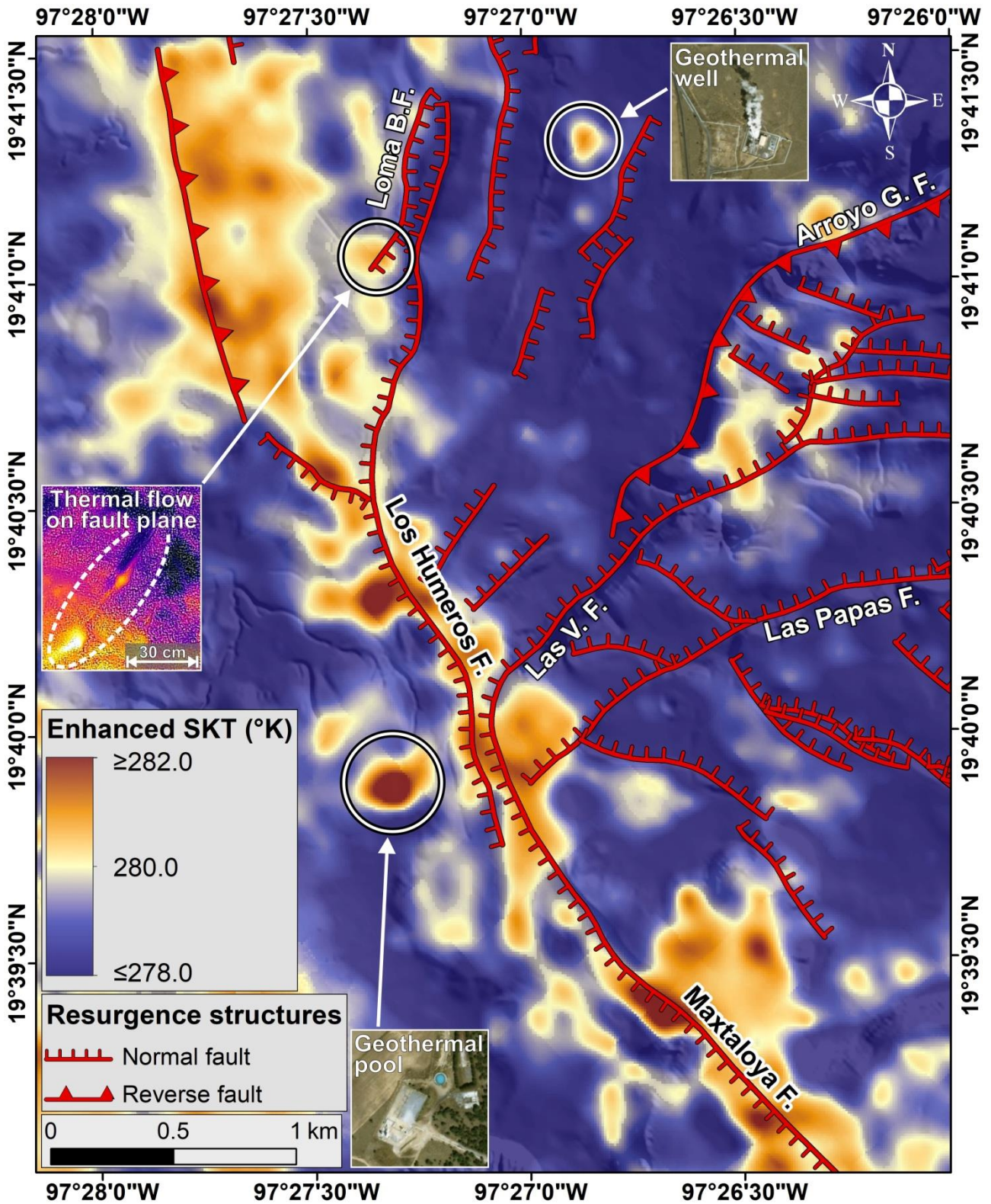
A — LH1732 (19° 39' 50.981" N, 97° 25' 44.558" W)

B — LH64 (19° 40' 25.108" N, 97° 25' 45.633" W)

C — LH62 (19° 40' 18.786" N, 97° 26' 6.535" W)

D — LH66 (19° 40' 38.931" N, 97° 26' 0.571" W)

E — LH23 (19° 40' 28.558" N, 97° 26' 38.304" W)

F — PDL52 (19° 40' 41.187" N, 97° 26' 35.606" W)

G — LH20 (19° 39' 15.969" N, 97° 26' 31.245" W)

H — PDL08 (19° 39' 2.290" N, 97° 26' 25.369" W)

Figure 2: photographs of faults in the Cuicuiltic Member along the structures mapped in Fig. 1.

Figure 3: enhanced surface kinetic temperature (SKT) of the Los Potreros caldera obtained from ASTER AST08 night–time thermal remote sensing data (see Norini et al., 2015, for details on methods and results). Examples of field–validated sources of thermal anomaly are shown in the insets (Norini et al., 2015, 2019). Thermal satellite data: credits LP-DAAC, USGS EROS data center at the NASA. Satellite images in the insets: credits Esri, DigitalGlobe, GeoEye.
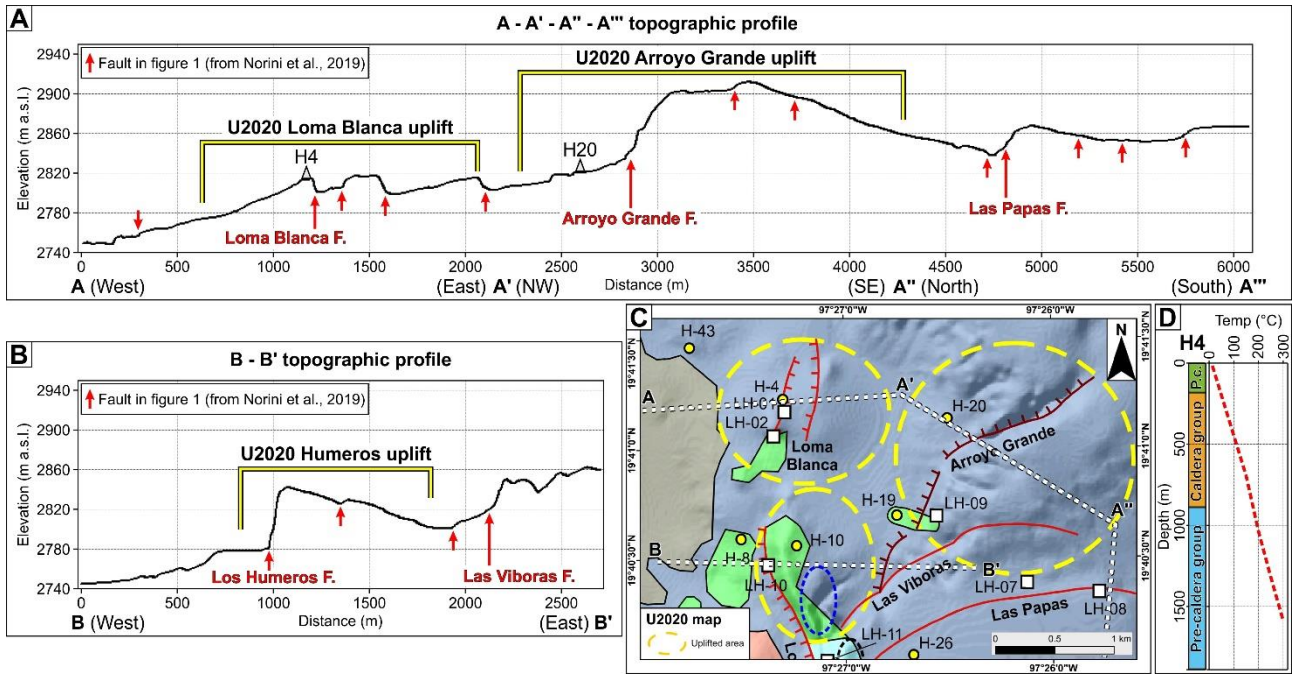
**Figure 4: topographic profiles along the (A) A–A'–A''–A''' and (B) B–B' traces shown in Fig. 1, and (C) schematic geological map (modified from U2020) outlining the three uplifted areas discussed by U2020; the traces of the two topographic profiles and the locations of the H4 and H20 well are also shown. (D) H4 lithological and temperature log (well data from Arellano et al., 2003, and U2020). P.c.: Post–caldera group.**
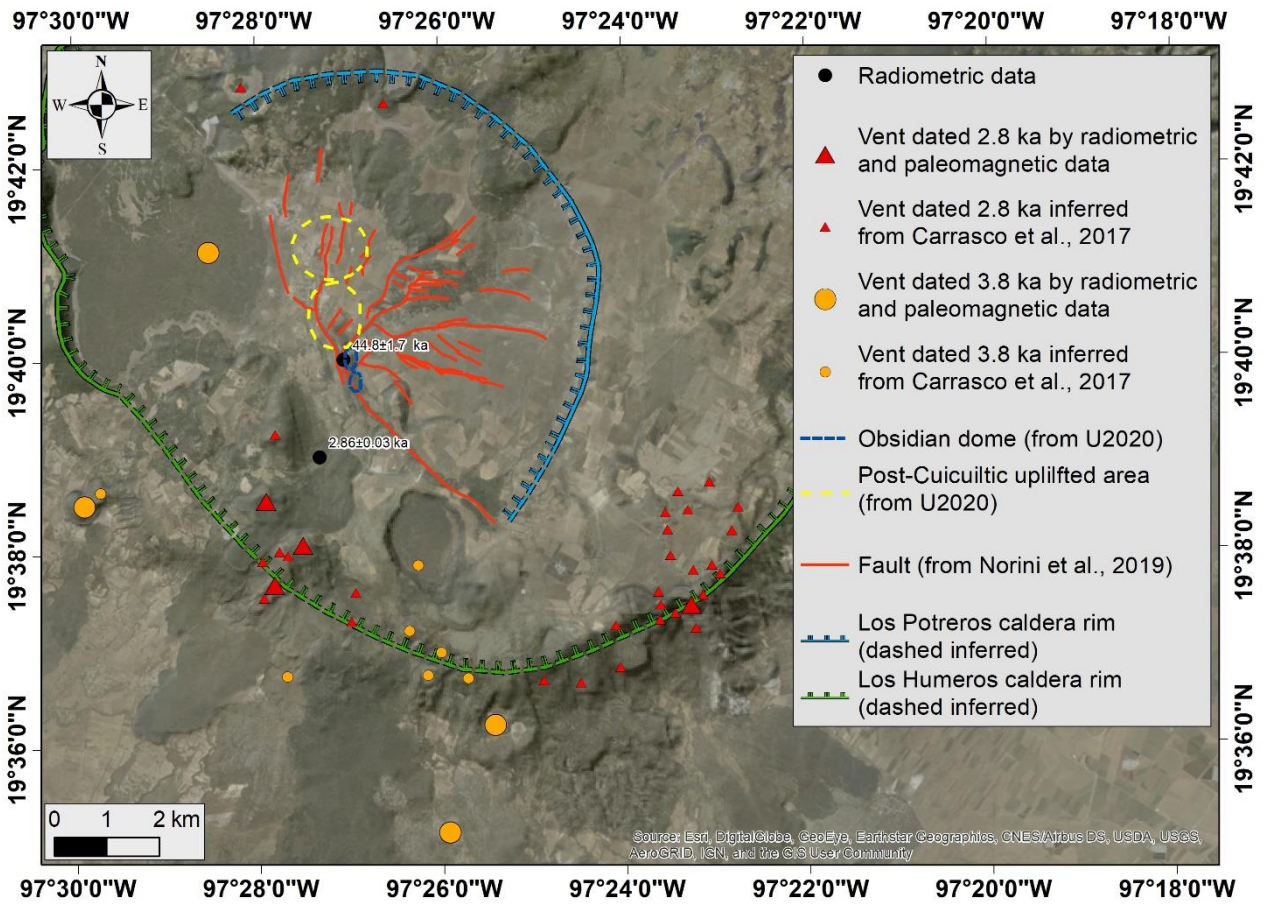
Figure 5: map of the post–Cuicuiltic Member vents and ages based on radiometric data, paleomagnetic analysis or inferred from geological map (Carrasco–Núñez et al., 2017, 2018; Juárez–Arriaga et al., 2018). The post–Cuicuiltic Member uplifted areas and obsidian dome proposed by U2020 are also shown. Active faults are from Norini et al. (2019).

Table 1 (supplementary data): field data of faults and fractures deforming the Cuicuiltic Member and the underlying units (see Fig. 1 for outcrops location).